

s-s*-d-wave superconductor on a square lattice and its BCS phase diagram

J. Ferrer, M. A. González-Alvarez

Departamento de Física, Facultad de Ciencias, Universidad de Oviedo, E-33007 Oviedo, Spain

J. Sánchez-Cañizares

Departamento de Física Teórica de la Materia Condensada, C-V, Universidad Autónoma de Madrid, E-28049 Madrid, Spain

We study an extended Hubbard model with on-site repulsion and nearest neighbors attraction which tries to mimic some of the experimental features of doped cuprates in the superconducting state. We draw and discuss the phase diagram as a function of the effective interactions among electrons for a wide range of doping concentrations. We locate the region which is relevant for the cuprates setting some constraints on the parameters which may be used in this kind of effective models. We also study the effects of temperature and orthorhombicity on the symmetry and magnitude of the gap function, and map the model onto a simpler linearized Hamiltonian, which produces similar phase diagrams.

(November 7, 2017)

Accurate results using a variety of experimental techniques like, for instance, ARPES,^{1,2} Josephson tunneling,³ penetration depth,⁴ or thermal conductivity measurements⁵ provide evidence on the d-wave symmetry of both the gap and order parameter functions of optimally doped and underdoped cuprates. Penetration depth measurements in slightly underdoped samples⁶ determined that their critical behavior fall on the 3D XY universality class (see also Refs. 7,8). This fact, which is not consistent with BCS weak coupling theory, indicates that the phase transition corresponds to the Bose-Einstein condensation of a single, complex order parameter field. The existence of a pseudogap with d-wave symmetry above the superconducting state for underdoped cuprates^{9–12} provides further confirmation on the non-BCS nature of the superconducting state.

There are several theoretical schemes which seem to fit into this experimental state of affairs: (a) In the magnetic scenario for the cuprates,^{13,14} the strong on-site repulsion among electrons gives rise to antiferromagnetic collective excitations. These degrees of freedom dress the bare interaction among the residual electrons, providing the pairing mechanism for the d-wave superconducting state and giving rise to the pseudogap in the normal state. (b) In some spin-charge separation theories,¹⁵ the pseudogap is related to the pairing of spinons and the superconducting state comes about when holons condense. (c) A further line of thought supposes that an undetermined high-energy pairing mechanism (which might be dressed vertex of case (a)) gives rise to an effective low energy pairing Hamiltonian where the coupling constants set the d-wave superconducting state in an intermediate coupling region.¹⁶

A thorough study of the phase diagram and qualitative features of a simple model which retain the electronic structure found in ARPES experiments is therefore an urgent task, if superconductivity in the cuprates has anything to do with scenarios (a) or (c). A BCS treatment of such a model should serve as a starting point for more accurate solutions which deal properly with the strong cor-

relations of the intermediate coupling regime.¹⁶ It should also be a useful tool for studies of transport, magnetic or optic properties of the cuprates, where bulk or surface impurities and other inhomogeneities must be taken into account.^{17–19}

We present in this article a detailed study of an effective pairing model, where the kinetic energy term comes from a tight-binding fit to the ARPES band structure of $\text{Bi}_2\text{Sr}_2\text{CaCu}_2\text{O}_{8+\delta}$ ($\text{Bi}2212$),²⁰ and we use either an attractive or repulsive on-site interaction plus a nearest-neighbors attraction term. In other words: we view the ARPES band structure of Ref. 20 as the low-energy pairing action of the actual Hamiltonian where the strong interactions among electrons, charge fluctuations, etc, have renormalized the kinetic energy and interaction terms giving rise to a set of hopping integrals, an effective on-site repulsion and a nearest-neighbors attraction, while other possible terms are irrelevant. The only channel which has not been dealt with in this kind of experimental implementation of the Renormalization Group is the superconducting one, so we need to perform only a conventional BCS decoupling scheme (the Hartree term would double-count interaction effects already taken into account). This model generates pure s and d, as well as mixed s+s*, s+s*+d and s+s*+id superconducting states in different regions of the phase diagram, where s* denotes an extended s state. We have performed most of our calculations at zero temperature where it is believed that the BCS approximation provides the gross features of the true ground state of the system, at least for small enough interactions.^{22,23}

We assume a tight-binding model on a squared lattice with a dispersion relation which keeps hopping terms up to five nearest neighbors

$$\xi(\vec{k}) = \sum_{i=1}^5 t_i \eta_i(\vec{k}) - \mu, \quad (1)$$

where the hopping integrals t_i and functions $\eta_i(\vec{k})$ are listed in table I of Ref. 20. The resulting electronic struc-

ture does not possess electron-hole symmetry and has a band width of about 1.1 eV. We vary μ to change the occupation number $n = 1 - x$ where x is the hole doping in the sample. The experimental evolution of the Fermi Surface (FS) with doping is not inconsistent with such a rigid shift of the band structure even though the ascription of a FS to a system with a pseudogap is a matter of controversy.²¹ We have also performed the calculations keeping only t_1 and t_2 , and obtained results quantitatively similar to those explained in this article.

The interaction term has an on-site potential, which can be either positive or negative plus a nearest neighbors attraction

$$V_{int}(\vec{k}\xi) = -V_0 - V_2(\cos(k_x\xi) + \cos(k_y\xi)), \quad (2)$$

where ξ is some typical length scale. This potential resembles the effective pairing interaction found in the magnetic scenario of the cuprates, if we set ξ equal to the magnetic coherence length (and slightly larger than the lattice spacing, see Figure 11 of Ref. 13).

The BCS expressions for the thermodynamic potential and gap functions are

$$\begin{aligned} \Omega(T, \mu) &= M \frac{|\Delta_s|^2}{V_0} + M \frac{|\Delta_{s^*}|^2 + |\Delta_d|^2}{V_2} + \\ &+ \sum_k \left[\xi_k - E_k - \frac{2}{\beta} \ln(1 + e^{-\beta E_k}) \right] \\ \Delta(\vec{k}) &= \Delta_s + \Delta_{s^*} F_{s^*}(\vec{k}) + \Delta_d F_d(\vec{k}), \end{aligned} \quad (3)$$

where M is the number of sites, $E_k = \sqrt{\xi_k^2 + |\Delta_k|^2}$ is the dispersion relation for the quasiparticles, and $F_{s^*,d} = \cos(k_x\xi) \pm \cos(k_y\xi)$.

The gap is a function of the dimensionless variable $k\xi$ for this particular choice of the interaction term, but we believe that such a radial dependence also holds for any potential of the form $V(\vec{k}\xi)$, even for moderate values of the coupling constants. In the magnetic scenario of the cuprates,¹⁴ ξ is the correlation length and, hence, the furnished gap function is not commensurate with the Brillouin zone and varies along with x . Plots of $\Delta(k)$ in the ΓM and MY directions for some underdoped and optimally doped Bi2212 samples,^{1,9} if possible, might demonstrate if this conjecture is correct. We set nevertheless ξ equal to the lattice spacing a throughout this paper.

The saddle point equations can now be easily written because the pairing interactions $V_{0,2}(k-k')$ are separable:

$$\begin{aligned} \Delta_s &= \frac{V_0}{M} \sum_k \frac{\Delta_k}{2E_k} \tanh\left(\frac{\beta E_k}{2}\right) \\ \Delta_{s^*,d} &= \frac{V_2}{M} \sum_k \frac{\Delta_k F_{s^*,d}}{2E_k} \tanh\left(\frac{\beta E_k}{2}\right) \end{aligned} \quad (4)$$

We compare the free energy per site of the different superconducting states $f(T, n) = \Omega(T, \mu(n))/M + \mu(n)n$, to ascertain their relative stability.

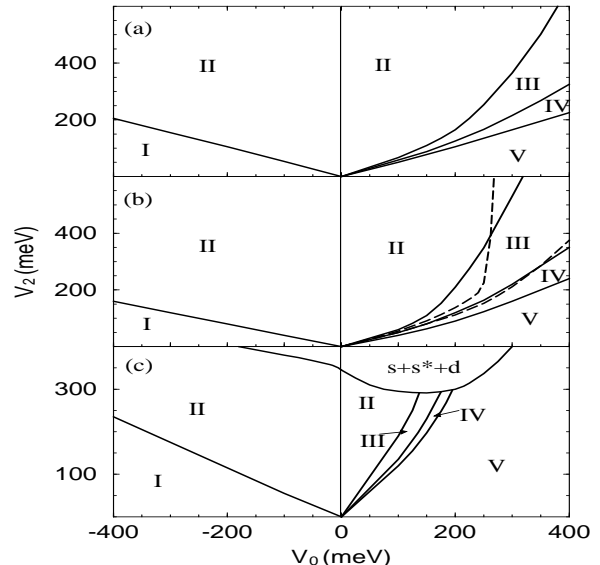


FIG. 1. Phase diagram for (a) $x = 0.05$ (b) $x = 0.2$ and (c) $x = 0.5$. Labels I, II and V denote the regions of metallic, d-wave and s+s* states, while in regions III and IV both d and s+s* solutions are found. The boundaries of the s+s*+id state are drawn only in figure (b), with dashed lines.

We examine first the phase diagram $[V_0, V_d]$ for x in the range $[0.0-0.5]$ in order to locate the region of parameter space which can be used to best represent the superconducting state of the cuprates. Figure 1 shows the phase diagrams for $x=0.05, 0.2$ and 0.5 . The coupled BCS equations possess only the trivial normal state solution in region I; only a pure d state solution in region II; only a mixed s+s* solution in region V, and only a pure s solution on the positive V_0 axis. There exist both pure d and mixed s+s* solutions in regions III and IV; the d state being more stable in region III and the mixed s+s*, in region IV. We also obtain a mixed s+s*+d solution for rather large values of V_2 , and a mixed s+s*+id state. These two states are always the most stable as long as they exist. The frontiers of stability of the different solutions change very slightly in the doping range $[0.05-0.4]$. When x exceeds 0.4, though, region II becomes increasingly thinner and localized around the V_2 axis. The only role of V_0 on the d-wave state is to set its domain of stability. In particular, the magnitude of Δ_d does not depend on it.

The size of the gaps as a function of hole concentration for pairs (V_0, V_2) inside regions II, IV and V is plotted in Figure 2. The three figures taken as a whole show that the d state is more stable only close to half-filling and for large enough values of the ratio V_2/V_0 , while the s states exist in the whole range of hole dopings. The shape of the curves for Δ_d is independent of V_0 ; V_2 only changes their height, so that one can write $\Delta_d = f(V_2)g(x)$. They always reach a peak at $x = 0.2$ and vanish at $x \pm 0.7$. The form of the curves for the s-state gaps does depend on both V_0 and V_2 , on the other hand, but its two maximums always occur at $x = 0.2$ and 0.8 . We find that

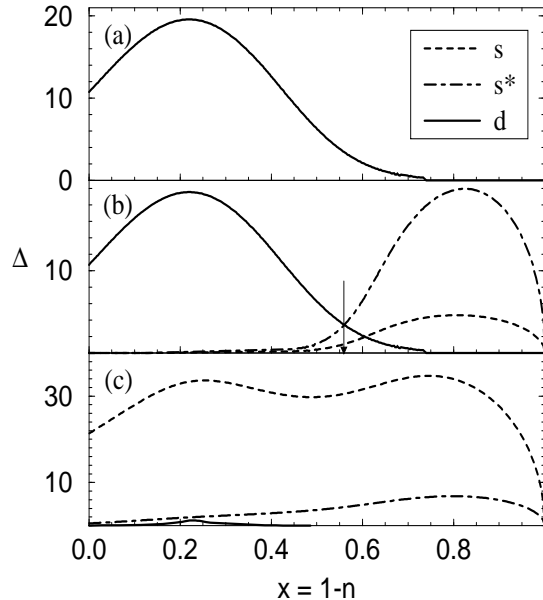


FIG. 2. Gaps (measured in meV) for (a) $V_0 = -250$, $V_2 = 150$ meV; (b) $V_0 = 50$, $V_2 = 150$ meV; and (c) $V_0 = 250$, $V_2 = 50$ meV.

the gaps of the $t_1 - t_2$ model have peaks at the same doping concentrations. We therefore conclude that their existence and position is due purely to filling effects and not to the peculiarities of the band structure. The arrow in Fig. 2(c) marks the boundary of stability x_c between the d and the s states, the free energy of the d state being lower for $x < x_c$.

There are compelling reasons to believe that the renormalized on-site interaction of this low energy model should still be strongly repulsive, so we focus our study on the negative V_0 quadrant now. A first point to notice is that the d-wave superconducting solution disappears for values of the on-site effective repulsion of the order of two times V_2 . This fact will set some constraints on the possible parent Hamiltonian of this model if it survives the inclusion of fluctuations over the Mean Field (MF) solution. Moreover, we estimate that the strength of the effective nearest neighbor attraction needed to obtain the experimental value of the gap for optimally doped Bi2212 (30 meV) is of about 140 meV, while V_0 can range from -320 to 0 meV. Such values, compared to a band width of 1.1 eV, place the resulting model within the weak coupling regime. This result leads to question the quantitative accuracy of the BCS gap and of the whole MF-RPA²² scheme at intermediate couplings even at $T = 0$. What actually happens is that such theories provide fine estimates for the gap and other physical magnitudes for large values of the coupling constants while for intermediate couplings and low dimensions, the results are much poorer. A comparison of MF theory and Bethe ansatz results for the 1d Hubbard model at half filling and $T = 0$ can be found in Ref. 24, where it is shown that the size of the gap is grossly overestimated by the MF solution at intermediate coupling.²⁵ We think that the gap should be estimated beyond MF-RPA theory in order to make

TABLE I. Changes in the gaps due to orthorhombicity for the case $V_0 = -250$ meV, $V_2 = 160$ meV and $x = 0.2$. Gaps are measured in meV.

α	β	Δ_d	Δ_s	Δ_{s^*}
0	0	22.1	0	0
0.05	0	20.5	-0.28	0.57
0	0.05	22.1	-0.23	1.54
0.05	0.05	20.6	-0.5	2.01
-0.05	0.05	20.4	0.07	0.86
0.05	-0.05	20.4	-0.07	-0.86
-0.05	-0.05	20.6	0.5	-2.01

direct comparisons with experiments. Such a theory will require much larger values of V_0 and V_2 to give a gap of 30 meV, thereby placing the coupling constants in the intermediate coupling regime.

The ratio $2\Delta_d(k_{F,max}, T = 0)/K_B T_d$ as a function of doping is non-universal and larger than the value obtained for a parabolic band (4.14). There is a plateau, which ranges from $x = 0.05$ to 0.4, where the ratio is almost constant and equal to 4.35, while it grows for smaller or larger doping, even reaching a value of 7 for $x = 0.65$.

The present model provides a universal value $x_0 = 0.2$ for optimal doping, defined as the hole concentration which yields the maximum critical temperature. We should caution however that experimentally, $\Delta_d(T = 0)$ and the temperature T^* at which the pseudogap begins to open up are monotonically decreasing functions of doping and do not peak at x_0 , while the experimental T_d has a maximum at about $x_0 = 0.15$.²⁶ RPA theories^{22,23} of s-wave superconductors, which permit to study the intermediate and strong coupling regimes find that electrons begin to pair up at a temperature T^* which is higher than the critical temperature T_c where pairs condense.

We study now how orthorhombicity effects can induce mixing of d and s states as might happen in YBCO, a cuprate where the a and b crystal axes become substantially inequivalent.³ In order to do so, we redefine the hopping integrals $t_{i,x,y} = t_i(1 \pm \alpha)$ for $i = 1, 3, 4$ so that the probability amplitude for electrons to leap between two sites depends on the spatial direction of the hop. We also suppose that the orthorhombicity leads to a different nearest neighbors interaction in the x and y directions, $V_{2,x,y} = V_2(1 \pm \beta)$. We find that a finite β doesn't modify much the d-wave gap, but indeed induces a finite s component (see table I). Orthorhombicity in the hopping integrals produces appreciable changes in Δ_d , but leads to smaller modifications in the s-state gaps. Notice finally how a sign change in α and/or β inverts the sign of the s components. This effect, which was already deduced phenomenologically using Ginsburg-Landau theory,^{27,28} implies that the s-wave component of the gap has opposite sign in different twin domains of twinned samples of YBCO. This is also the explanation given for the Fraunhofer pattern observed in a recent c-axis Josephson tun-

ACKNOWLEDGMENTS

The authors gratefully acknowledge financial support from the Spanish Dirección General de Enseñanza Superior, Project No. PB96-0080-C02.

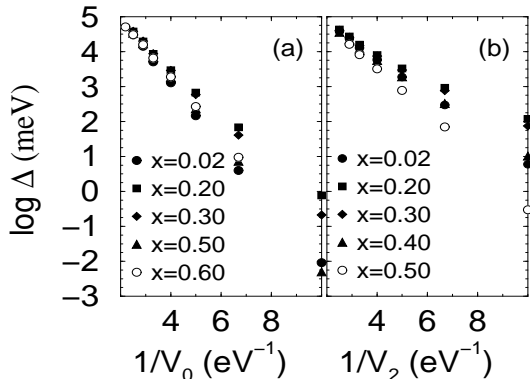


FIG. 3. (a) $\log \Delta_s$ versus $1/V_0$ for $V_2 = 0$ and several x . (b) $\log \Delta_d$ versus $1/V_2$ for $V_0 = 0$.

neling experiment, where the junction had been grown across a single twin boundary.²⁹

One may compare the results obtained within this tight-binding model with the predictions of a much simpler isotropic Hamiltonian, with a linearized dispersion relation and pairing interaction of the form

$$\xi_k = \frac{\hbar^2 k^2}{2m} - \mu \simeq \hbar v_F (k - k_F)$$

$$V(\vec{k} \pm \vec{k}') \simeq -V_0^L - V_2^L \cos(2\theta) \cos(2\theta') \quad (5)$$

In this case, the gap function $\Delta^L = \Delta_s^L + \Delta_d^L \cos(2\theta)$ obeys the following saddle point equations³⁰

$$\Delta_{s,d}^L = g^L V_{0,2}^L \int_0^{2\pi} \frac{d\theta}{2\pi} \int_0^{E_D} d\varepsilon \frac{F_{s,d}^L(\theta) \Delta^L(\theta)}{\sqrt{\varepsilon^2 + |\Delta^L(\theta)|^2}}, \quad (6)$$

where $F_s^L = 1$, $F_d^L = \cos(2\theta)$, and g^L is the two-dimensional density of states. Now, expanding Eq. (4) up to order $(k\xi)^4$ and comparing with Eq. (6), we obtain the following relations: $g^L V_0^L = g V_0$, $g^L V_2^L = \gamma^2 g V_2$, $\Delta_s^L = \Delta_s$ and $\Delta_d^L = \gamma \Delta_d$, where g is an effective tight-binding density of states and $\gamma = -(k_F \xi)^2 / 2 + (k_F \xi)^4 / 24$. These two parameters, together with the cut-off E_d , can be used to fit $\Delta_{s,d}$ with $\Delta_{s,d}^L$ along the V_0 and V_2 axes, respectively. As shown in Fig. 3, we indeed find linear behavior for $\log \Delta$ as a function of $1/V$, from which we extract values of $k_F \xi / \pi$ ranging from 1.21 to 1.27, and g from 1.1 to 1.6 eV^{-1} .

In conclusion, we have proposed and studied an effective tight-binding model for the superconducting state of the cuprates, guided mostly by results of ARPES experiments. In particular, we have delineated its weak-coupling phase diagrams for different hole doping concentrations close to the experimental optimum doping. We have been able to establish the region of parameters which is likely to be relevant for the cuprates in absolute energy units (meV). We have finally mapped the tight-binding model onto a much simpler linearized model and obtained similar phase diagrams.

- ¹ H. Ding *et al.*, Phys. Rev. B **54**, R9678 (1996).
- ² J. M. Harris *et al.*, Phys. Rev. Lett. **79**, 143 (1997).
- ³ J. Annett, N. Goldenfeld, and A. J. Leggett, in *Physical Properties of High Temperature Superconductors V*, edited by D. M. Ginsberg (World Scientific, New Jersey, 1996).
- ⁴ C. Panagopoulos *et al.*, Phys. Rev. Lett. **79**, 2320 (1997).
- ⁵ H. Aubin *et al.*, Phys. Rev. Lett. **78**, 2624 (1997).
- ⁶ S. Kamal *et al.*, Phys. Rev. Lett. **73**, 1845 (1994).
- ⁷ Y. J. Uemura, condmat/9706151 (unpublished).
- ⁸ V. J. Emery and S. A. Kivelson, Nature **374**, 434 (1995).
- ⁹ A. G. Loeser *et al.*, Science **273**, 325 (1996).
- ¹⁰ H. Ding *et al.*, Nature **382**, 51 (1996).
- ¹¹ A. V. Puchkov, P. Fournier, T. Timusk, and N. N. Kolesnikov, Phys. Rev. Lett. **77**, 1853 (1996).
- ¹² T. Watanabe, T. Fujii, and A. Matsuda, Phys. Rev. Lett. **79**, 2113 (1997).
- ¹³ D. J. Scalapino, Physics Reports **250**, 330 (1995).
- ¹⁴ A. V. Chubukov, D. Pines, and B. P. Stojkovic, J. Phys. Condens. Matter **8**, 10017 (96).
- ¹⁵ X. G. Wen and P. A. Lee, Phys. Rev. Lett. **76**, 503 (1996).
- ¹⁶ J. Engelbrecht, A. Nazarenko, M. Randeria, and E. Dagotto, condmat/9705166 (unpublished).
- ¹⁷ A. V. Balatsky and M. I. Salkola, Phys. Rev. Lett. **76**, 2386 (1996).
- ¹⁸ P. M. A. Cook, R. Raimondi, and C. J. Lambert, Phys. Rev. B **54**, 9491 (1996).
- ¹⁹ W. C. Wu, B. W. Statt, Y.-W. Hsueh, and J. P. Carbotte, Phys. Rev. B **56**, R2952 (1997).
- ²⁰ M. R. Norman, M. Randeria, H. Ding, and J. C. Campuzano, Phys. Rev. B **52**, 615 (1995).
- ²¹ H. Ding *et al.*, Phys. Rev. Lett. **78**, 2628 (1997).
- ²² J. R. Engelbrecht, M. Randeria, and C. A. R. Sá de Melo, Phys. Rev. B **55**, 15153 (1997).
- ²³ V. M. Loktev and S. G. Sharapov, condmat/9706285 (unpublished).
- ²⁴ J. Ferrer, Phys. Rev. B **51**, 8310 (1995).
- ²⁵ The main role of RPA is to incorporate the collective modes to the MF solution; RPA corrections therefore diverge in 1d even at $T = 0$ because of the Mermin-Wagner theorem.
- ²⁶ H. Ding *et al.*, condmat/9712100 (unpublished).
- ²⁷ M. Sigrist *et al.*, Phys. Rev. B **53**, 2835 (1996).
- ²⁸ M. E. Zhitomirsky and M. B. Walker, Phys. Rev. Lett. **79**, 1734 (1997).
- ²⁹ K. A. Kouznetsov *et al.*, Phys. Rev. Lett. **79**, 3050 (1997).
- ³⁰ K. A. Musaelian, J. Betouras, A. V. Chubukov, and R. Joynt, Phys. Rev. B **53**, 3598 (1996).